Hydrochemical evolution and water quality along the groundwater flow path in the Sandıklı plain, Afyon, Turkey

M. Afşin

Abstract An unconfined aquifer system suggests an open system in the study area. Hydrochemical evolution is related to the flow path of groundwater. The groundwaters are divided into two hydrochemical facies in the study area, 1) Ca–Mg–HCO$_3$ and 2) Ca–Mg–SO$_4$HCO$_3$. Facies 1 has shallow (young) waters which dominate in recharge areas during rapid flow conditions, whereas facies 2 may show shallow and mixed waters which dominate intermediate or discharge areas during low flow conditions. Ionic concentrations, TDS, EC and water quality are related to groundwater residence time and groundwater types. The groundwaters in the plain are chemically potable and suitable for both domestic and agricultural purposes.

Key words Hydrochemical evolution · Unconfined aquifer · Facies · Shallow water · Residence time

Introduction

The Sandıklı plain is located to the southeast of Afyon, Turkey (Fig. 1). Some studies have been carried out on the geological and hydrogeological features of the area by Bulutçu (unpublished data), Öztaş (unpublished data) and Afşin (1991). The relationship between groundwater flow, hydrogeologic properties and hydrochemistry has been studied by many researchers (Back 1960, Schoeller 1962, Domenico 1972, Freeze and Cherry 1979, Ophori and Tóth 1989, Domenico and Schwartz 1990, Bayarı and Kurttaş 1995). The chemical composition of the groundwater which moves from the recharge area to the discharge area reflects changes by various geochemical p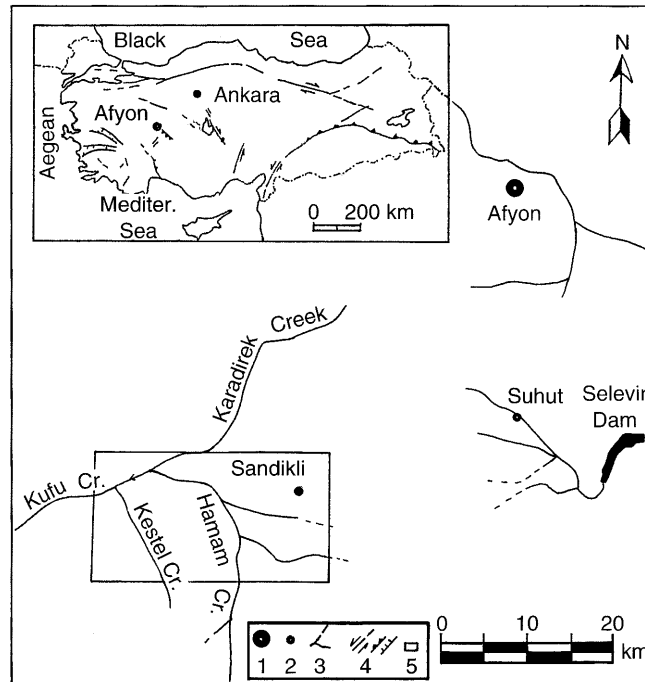rocesses. Dissolved and colloidal solids, and organisms in groundwater provide information about the geology of the recharge area, flow paths and environment.

The aims of this study are to explain the interactions between rock and water, to separate hydrochemical facies, and to confirm the effect of ion exchanges on groundwater quality along the groundwater flow path in the unconfined aquifer by using chemical analyses. An overall evaluation of chemical results from 38 water samples from different boreholes (20), springe (15) and crecks (3) in the area and vicinity were selected and analyzed in the laboratory (Ankara University). All parameters, except temperature, have been measured in the laboratory following a delay of one week. The results of the analyses were compared to WHO (1984), Turkish Standard Institution (TSI, 1986) and Water Pollution Control Act (WPA, 1988) water quality guidelines. These results show that almost all waters can be considered as having permanently drinkable, very good and high quality waters.

M. Afşin (✉)
Geological Engineering Department, Nigde University, Aksaray 68100, Turkey

Fig. 1
Location map of the study area **1** province capital, **2** county town, **3** perennial and seasonal creek or stream, **4** defined faults (possible etc.), **5** study area
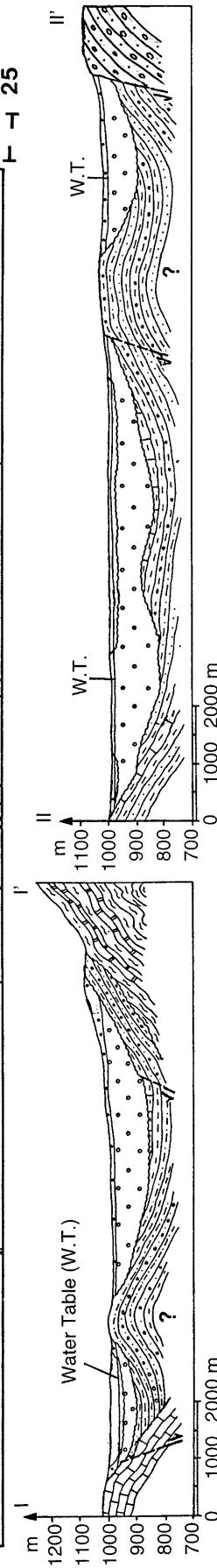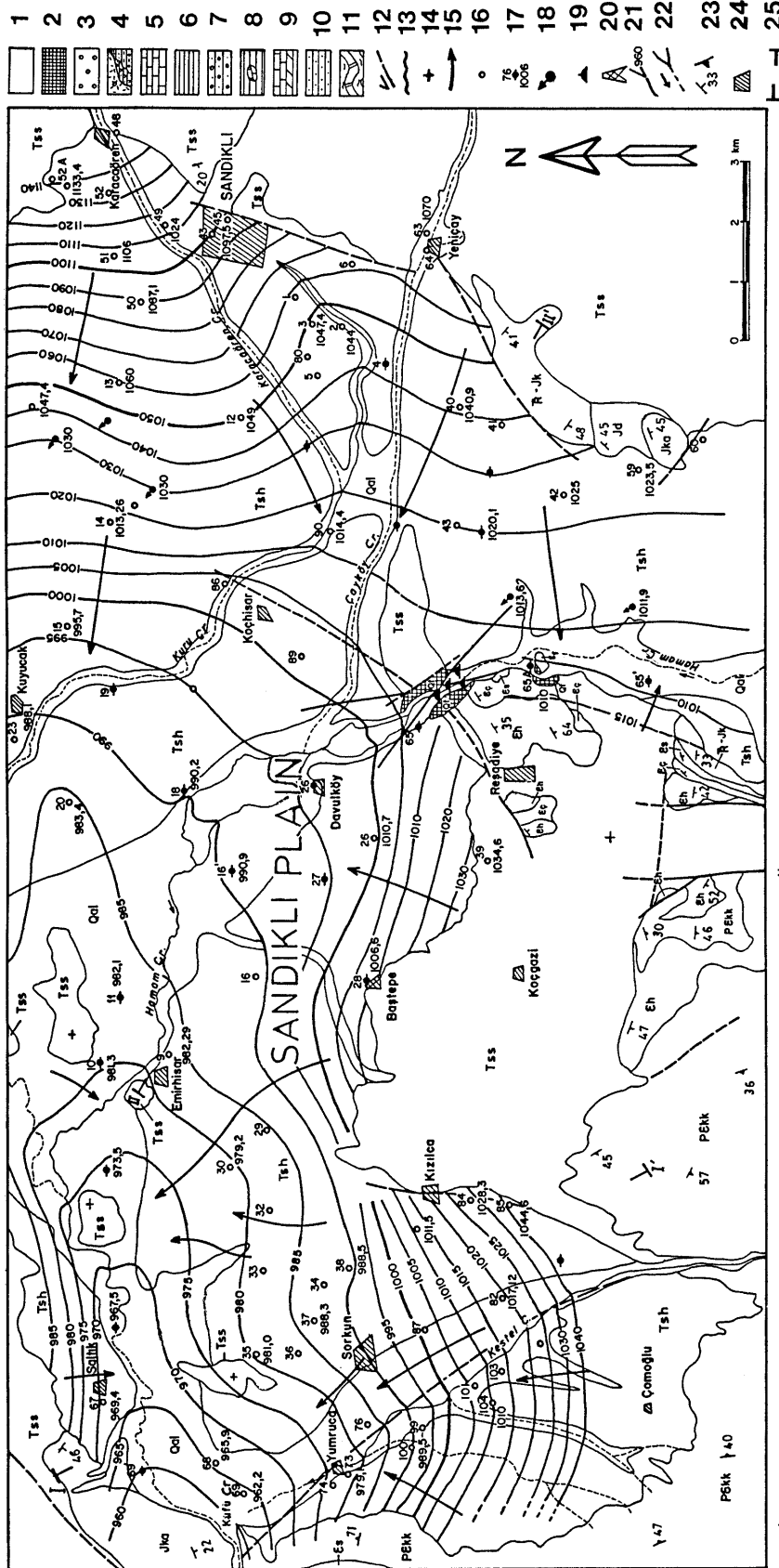
Fig. 2
Hydrogeologic map and cross-sections of the study area 1 Alluvium (Qal), 2 Travertine (Qtr), 3 Pliocene (Tsh), 4 Upper Miocene (Tss), 5 Upper Jurassic-Lower Cretaceous (Jka), 6 Lower Jurassic (Jd), 7 Upper Triassic-Lower Jurassic (Tʀ-Jk), 8 Upper Cambrian-Lower Ordovician (∈s), 9 Middle Cambrian (∈ç), 10 Lower Cambrian (∈h), 11 Precambrian (P∈kk), 12 fault (possible etc.), 13 unconformity, 14 horizontal bed, 15 groundwater flow direction, 16 sweep well, 17 well number/static level, 18 spring, 19 hot-mineral spring (Hudai Bath), 20 drilling well, 21 groundwater contour level (Possible etc.), 22 perennial/seasonal creek, 23 strike and dip of bed/foliation, 24 Settlement, 25 line of the hydrogeologic cross-section

Hydrogeology

The exposed lithological units of the Sandıklı plain range in age from Precambrian to Quaternary and have different hydrogeological characteristics (Fig. 2). The units of similar hydrogeological characteristics are summarized in Table 1 and qualitatively grouped as impermeable, semipermeable and permeable. In the study area, the Kocayayla and Seydişehir Formations are impermeable, and the Hudai and Çaltepe Formations are semipermeable. The Karakaya and Akdağ Formations are permeable and disconformably overlie the previously mentioned units. At the top of the sequence, the Sandıklı Formation is semipermeable, and lies above another disconformity. The Hamamçay Formation, travertine and alluvium are permeable. Clayey layers in Pliocene lacustrine sediments are impermeable, but weakly cemented conglomerate and sandstone layers are permeable. The Travertines have secondary porosity because of hydrothermal karstification.

The Sandıklı plain is filled with Pliocene–Quaternary-aged units. These materials are composed of weakly cemented conglomerate and sandstone with sand, sandy gravel, and clay lenses. The results of drill wells indicate that the thickness of the alluvium aquifer is approximately 200 m. The thickness increased in the middle, south and north-northwest of the plain where creeks joined each other. The porosity and permeability values vary from 20%–40%, and 1.0×10^{-3}–8.6×10^{-5} m/s in the Hamamçay Formation; and 24%–32%, and 1.1×10^{-3}–1.8×10^{-3} m/s in the alluvium, respectively (Afşin 1991). The general flow direction of the aquifer water is from E-SE to W-NW. The Hamamçay Formation and alluvium units form unconfined and confined aquifers under suitable hydraulic conditions. Here, an unconfined aquifer has been considered. The unconfined aquifer system in the study area suggests an open system. This situaton affects the groundwater flow system and residence time. Unlimited CO_2 may be supplied under open-system dissolution conditions. In unconfined aquifers, as long as the infiltration from recharge water continues, there would be a continuous or fixed supply of CO_2 gas dissolved in groundwater (Bayarı and Kurttaş 1995). The major source of carbon dioxide results from the organic reactions taking place in the root zone (Appelo and Postma 1992). The unconfined aquifer of the Sandıklı plain is open to recharge from precipitation, and a continuous CO_2 input along the flow path allows perpetual dissolution of carbonate mineral. Organic matter oxidation which leads to carbon dioxide production in the aeration zone may be an important reaction in the unconfined section of the Sandıklı plain.

Hydrochemical evaluation

Results and discussion

The mean air temperature of the study area is 12.4 °C and the mean values of the temperature, pH, electrical con-

Table 1
Stratigraphic relations of the geologic units in the study area showing hydrogeologic properties

Age	Formation	Hydrogeologic properties
Quaternary	Alluvium (Qal) Travertine (Qtr)	permeable (Alluvium aquifer)
Pliocene	Hamamçay Formation (Tsh)	permeable
Upper Miocene	Sandıklı Formation (Tss) volcanic rocks (andesite, tuff) lacustrine sediments (conglomerate, clay, marl)	semipermeable
Upper Jurassic–Upper Cretaceous	Akdağ Formation (Jk-a) (limestone)	permeable
Lower Jurassic	Derealanı Formation (Jd) (siltstone, marl)	impermeable (aquiclude)
Upper Triassic–Lower Jurassic	Karakaya Formation (TR-Jk) (conglomerate)	permeable
Upper Cambrian–Lower Ordovician	Seydişehir Formation (∈s) (shale)	impermeable
Middle Cambrian	Çaltepe Formation (∈ç) (dolomite, limestone)	semipermeable
Lower Cambrian	Hudai Formation (∈h) (quartzite)	semipermeable
Precambrian	Kocayayla Formation (P∈kk) (schist, marble)	impermeable

ductivity (EC) and total dissolved solids (TDS) of the waters are 11.2 °C, 8.2, 610 μmho/cm, and 348.6 mg/l, respectively (Fig. 3a, b; Table 2).

The interplay of precipitation and dissolution processes serves as an important determining factor of the overall chemical character of the groundwater coming from the unconfined aquifer. Some ionic parameters were used to identify the plotting order of the samples due to the enrichment of the ionic composition with increasing length of groundwater flow path. The Ca^{2+}, Mg^{2+}, HCO_3^- and SO_4^{2-} ions are generally found at higher concentrations compared to the other ions (Na^+, K^+, Cl^-) in the groundwaters of the Sandıklı plain. The dissolution of carbonate rocks enriches the water in Ca^{2+} and Mg^{2+} ions. The Ca^{2+} probably originates from the decomposition of albite in the volcanic rocks.

A sharp increase in HCO_3^- values is observed from some water samples, 52A, 65A, and 100 (Fig. 4a, b). These data may illustrate the dissolution of volcanics and limestones in the recharge area due to the acidic precipitation (Bayarı and Kurttaş 1995) and ionic enrichment. Carbonate values are high near limestone and low around volcanic and metamorphic rocks. The major anion, HCO_3^-, of the groundwaters in the recharge areas is formed through the dissolution of $CaCO_3$ by CO_2-rich meteoric water infiltrating along groundwater flow paths. The carbonate mineral dissolution may be diminished during the travel of groundwater from the recharge areas towards the thicker parts of the aquifer because of the lack of carbon dioxide.

A decrease in ionic concentration which was representative of the dissoluton of the parent rock was observed near metamorphic rock at the beginning of the Kestel
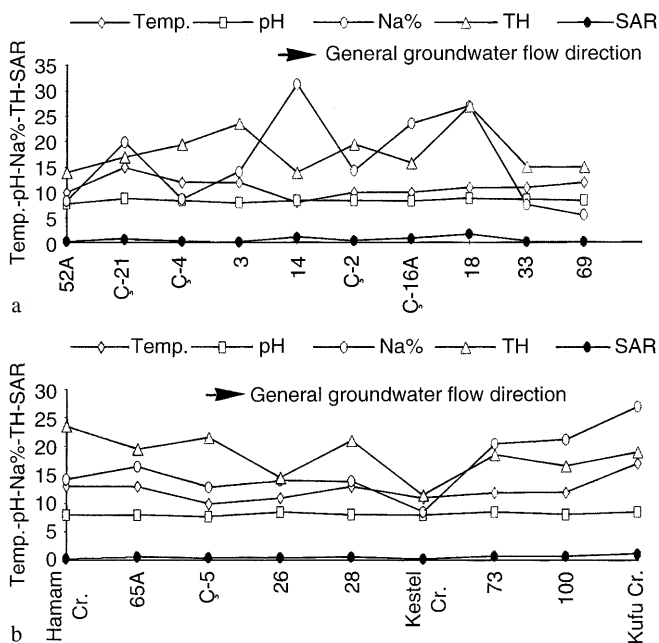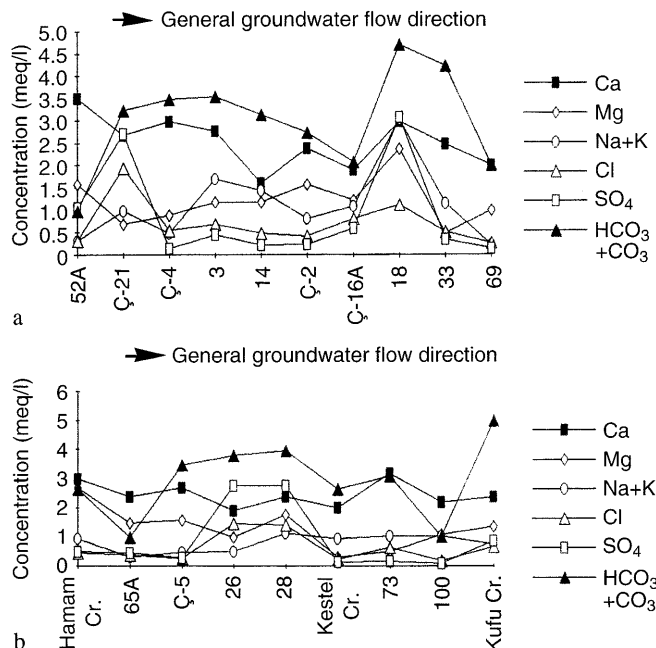
Fig. 4a, b
Variation of ionic composition along the groundwater flow path (units are as in Table 2)

creek (Fig. 6b). The source of Mg^{2+} in the waters may be the decomposition of biotite, hornblende and pyroxene in the volcanics (Afşin and Baş 1996). The Na^+ and K^+ values are relatively high in groundwaters (Ç-21, 3, 18) beneath the northeastern portion of the Sandıklı plain (Fig. 4a, b). The Na^+ probably comes from the decomposition of albite feldspar. An increase in Na^+ and K^+ is assumed to result from cation exchange of Ca^{2+} and Mg^{2+} ions by mineral-water interaction. For this reason, there is a positive correlation (r = 0.34) between Ca^{2+} and Mg^{2+} ions.

The waters generally in the NW, NE and central sections of the plain are enriched in SO_4^{2-} anions. This may be evidence of mixing of water from the Miocene-aged unit (Sandıklı Formation) or sulfide (pyrite) oxidation since the unit contains coal layers in the NE of Sandıklı (Afşin 1991). The SO_4^{2-} contribution from pyrite oxidation is neglected. Increasing Ca^{2+} with decreasing Na^+ may correspond to a prolonged contact time with clay, i.e., ion exchange, in the aquifer. An increase in ionic concentration observed in some wells (18, 26, 29, 33, 73) may suggest a transition zone between shallow and deep circulation because of the thickness of the aquifer. In these wells, Ca^{2+}, Mg^{2+} and HCO_3^- values are high (Figure 4a, b). There are positive and highly positive correlations between $Cl^--SO_4^{2-}$ (r = 0.85), $Mg^{2+}-Na^+$ (r = 0.62) and $Cl^--HCO_3^-$ (r = 0.64) ion pairs (Table 3).

As groundwater moves along its flow paths in the saturated zone, the TDS values increase and most of the major ions normally occur (Freeze and Cherry 1979). The TDS, EC, Ca^{2+}, HCO_3^- and SO_4^{2-} values increase towards the middle of the plain along the groundwater flow direc-

Fig. 3a, b
Variation of some physical and chemical parameters along the groundwater flow path (shallow flow, units are as in Table 2)

Table 2
Physical and chemical data used in the study [Concentrations in meq/l, Temp=temperature (°C), EC=electrical conductivity (μmho/cm), TDS=total dissolved solids (mg/l), SI=saturation index (ca=calcite, do=dolomite, gy=gypsum), TH=total hardness (French), SAR=sodium adsorption ratio, logpCO₂ (Atm.). (Data source: Afşin 1991)

No(Field No)	Ca	Mg	Na	K	Cl	SO₄	HCO₃	CO₃	Ca/Na	Ca/Mg	SO₄/Cl	Temp.	pH	EC	Na%	SAR	TH	TDS	SIca	SIdo	SIgy	log pCO₂	Facies
1(2)	3.49	1.58	2.15	0.75	1.04	3.21	1.4	0.38	1.62	2.21	3.09	9	8.4	771	26.9	1.35	25.5	467					Ca-Mg-SO₄-HCO₃
2(3)	2.79	1.18	1.6	0.1	0.68	0.45	2.46	1.08	1.74	2.36	0.66	12	8	451	14.2	0.22	23.5	306	0.43	0.36	-4.13	-3	Ca-Mg-HCO₃
3(14)	1.6	1.18	1.33	0.11	0.48	0.23	3.15		1.2	1.35	0.48	8	8.4	520	31.4	1.12	14	302	0.64	1.26	-5	-3.2	Ca-Mg-HCO₃
4(15)	2.0	0.99	1.05	0.02	0.81	0.1	2.61	0.3	1.9	2.02	0.12	9	8.1	484	25.8	0.86	15	287	0.46	0.72	-5.24	-3	Ca-Mg-HCO₃
5(18)	2.99	2.37	2.99	0.05	1.11	3.08	3.61	1.1	1.0	1.26	2.77	11	8.7	1130	27	1.77	27	630	1.45	1.45	-3.68	-3.4	Ca-Mg-HCO₃
6(18A)	3.89	1.87	3.05	0.35	0.51	0.66	2.47	1.0	1.27	2.08	1.29	10	8.5	558	33.2	1.79	29	445					Ca-Mg-HCO₃
7(26)	1.9	0.99	0.48	0.02	1.47	2.77	2.79	1.0	3.96	1.92	1.88	11	8.6	1229	14.1	0.4	14.5	476	1.09	1.06	-4.83	-3.3	Ca-Mg-SO₄-HCO₃
8(28)	2.39	1.78	0.75	0.39	1.41	2.77	3.29	0.67	3.19	1.34	1.96	13	8.1	1410	14	0.52	21	527	0.58	0.65	-3.84	-2.8	Ca-Mg-HCO₃
9(33)	2.49	0.49	0.25	0.05	0.52	0.34	3.44	0.8	9.96	5.08	0.65	11	8.6	585	7.58	0.2	15	351					Ca-Mg-HCO₃
10(35)	1.95	1.82	0.46	0.01	0.57	0.09	3.0	0.32	4.24	1.07	0.16	11	7.8	642	10.8	0.34	19	299	0.19	-0.27	-5.33	-2.5	Ca-Mg-SO₄-HCO₃
11(44)	2.89	0.49	0.61	0.01	0.93	1.05	0.52		4.74	5.9	1.13	12	7.1	500	15.2	0.47	17	193	-1.17	-1.5	-4.08	-2.6	Ca-Mg-HCO₃
12(51)	1.0	0.59	0.5	0.05	0.29	0.82	0.95	0.68	2.0	1.69	2.83	8	7.4	292	23.3	0.56	8	189					Ca-Mg-SO₄-HCO₃
13(52)	1.6	0.99	0.38	0.09	3.91	8.18.	5.97	0.83	4.21	1.62	2.09		7.6	2000	12.4	0.33	13	1000					Ca-Mg-SO₄-HCO₃
14(52A)	1.8	0.99	0.28	0.03	0.31	1.06	0.98		6.43	1.82	3.42	10	7.8	402	8.26	0.24	14	177	-0.33	-0.4	-4.26	-3.1	Ca-Mg-SO₄-HCO₃
15(65A)	2.39	1.48	0.78	0.06	0.37	0.44	0.8		3.06	1.61	1.19	13	7.9	520	16.5	0.56	19.5	169	0.26	-0.31	-4.55	-3.2	Ca-Mg-HCO₃
16(69)	2.0	0.99	0.18	0.04	0.27	0.14	2.0		11.11	2.02	0.52	12	8.5	261	5.59	0.15	15	211	0.64	0.55	-5.15	-3.5	Ca-Mg-HCO₃
17(73)	3.19	0.49	0.97	0.08	0.64	0.16	3.08		3.29	6.51	0.25	12	8.5	572	20.4	0.71	18.5	291	0.87	0.48	-4.97	-3.3	Ca-Mg-HCO₃
18(76)	1.2	0.74	0.17	0.03	0.37	0.11	0.98		7.06	1.62	0.3	11	8.1	234	7.91	0.17	9.75	116	-0.23	-0.27	-5.97	-3.4	Ca-Mg-HCO₃
19(87A)	3.39	1.97	1.7	0.24	0.45	0.13	4.7		1.99	1.72	0.29	12	8.4	514	23.2	1.04	27	450	1.12	0.56	-4.99	-3	Ca-Mg-HCO₃
20(100)	2.2	1.08	0.92	0.11	0.2	0.09	1.02		6.09	5.18	0.45	12	8.1	106	21.7	0.72	16.5	149	-0.12	-0.26	-5.27	-3.4	Ca-Mg-HCO₃
21(C-2)	2.39	1.58	0.7	0.11	0.43	0.24	2.51	0.58	3.41	1.51	0.56	10	8.7	424	14.8	0.5	20	298					Ca-Mg-HCO₃
22(C-2B)	2.49	1.38	0.64	0.01	0.32	1.4	2.51		3.89	1.8	4.37	10	8.4	424	14.1	0.46	19.5	313	0.74	0.67	-3.9	-3.3	Ca-Mg-HCO₃
23(C-4)	2.99	0.89	0.38	0.1	0.54	0.14	3.16	0.32	7.87	3.36	0.26	12	8.5	499	8.68	0.27	19.5	321	1.06	0.35	-4.69	-3.2	Ca-Mg-HCO₃
24(C-5)	2.69	1.58	0.65	0.08	0.25	0.28	2.44	0.38	4.14	1.7	1.12	10	7.7	471	12.9	0.44	21.5	152	0.13	0.07	-4.7	-2.5	Ca-Mg-HCO₃
25(C-7)	1.8	1.18	0.26	0.05	0.29	0.32	2.77		6.92	1.52	1.1	9	8.6	424	7.85	0.21	15	252					Ca-Mg-HCO₃
26(C-9)	2.49	0.44	0.31	0.08	0.2	0.32	3.34		8.03	5.66	1.6	12	8.3	505	9.28	0.18	14.7	292	0.77	0.45	-4.52	-3	Ca-Mg-HCO₃
27(C-10)	1.3	0.59	0.19	0.03	0.26	0.16	1.58		6.84	2.2	0.61	11	8.6	261	8.96	0.19	9.5	152	0.55	-0.15	-5.05	-3.7	Ca-Mg-HCO₃
28(C-16A)	1.9	1.22	1.0	0.08	0.8	0.59	1.85	0.24	1.9	1.56	0.74	10	8.35	389	23.6	0.8	15.8	264					Ca-Mg-HCO₃
29(C-16B)	1.6	0.99	0.61	0.11	0.86	0.21	1.85		2.62	1.62	0.24	10.5	8.1	332	15.9	0.53	13	213	0.43	1.01	-5.03	-3.1	Ca-Mg-HCO₃
30(C-17)	2.09	1.02	1.24	0.11	0.41	0.13	2.39	0.64	1.68	2.05	0.32	11	7.5	367	27.2	0.97	16.5	332	-0.15	-0.21	-5.17	-2.3	Ca-Mg-HCO₃
31(C-18)	1.3	0.59	0.18	0.08	2.84	0.65	3.38		7.22	2.2	0.27	13	8.3	807	8.33	0.18	9.5	363	0.56	0.95	-4.61	-3.1	Ca-Mg-SO₄-HCO₃
32(C-20)	1.7	0.59	0.52	0.09	2.84	8.82	8.46		3.27	2.88	3.1	11	8.7	2000	17.9	0.49	11.5	1097					Ca-Mg-SO₄-HCO₃
33(C-21)	2.69	0.69	0.87	0.1	1.95	2.71	2.7	0.54	3.09	3.9	1.39	15	8.8	316	19.91	0.67	17	482	1.27	1.03	-3.75	-3.5	Ca-Mg-HCO₃
34(C-28)	2.39	1.13	0.33	0.01	0.76	0.17	4.75		7.24	2.11	0.22		7.8	562	8.48	0.3	17.7	396	0.11	0.01	-4.93	-2.7	Ca-Mg-HCO₃
35(C-29)	2.19	1.58	0.43	0.09	0.42	0.54	2.79	0.8	5.09	1.39	1.28	10	8.6	537	9.95	0.31	19	336					Ca-Mg-HCO₃
36(Hamam Cr.)	2.99	1.68	0.8	0.15	0.46	0.5	1.64	1.0	3.74	1.78	1.09	13	8	451	14.2	0.22	23.5	306	0.43	0.36	-4.13	-0.8	Ca-Mg-HCO₃
37(Kestel Cr.)	2.0	0.3	0.22	0.04	0.24	0.15	2.11		9.09	6.67	0.62	11	8	217	8.59	0.2	11.5	195	0.2	-0.16	-5.05	-2.9	Ca-Mg-HCO₃
38(Kufu Cr.)	2.39	1.38	1.44	0.09	0.67	0.88	2.65	0.72	1.66	1.73	1.31	17	8.6	617	27	1.04	19	373	1.11	0.84	-4.25	-3.4	Ca-Mg-HCO₃

Table 3
Correlation coefficients (r) for the hydrochemical data

	Ca	Mg	Na	K	Cl	SO_4	HCO_3	CO_3	Ca/Na	Ca/Mg	SO_4/Cl	Temp.	pH	EC	NA%	SAR	TH	TDS	SICa	SIdo	SIgy
Mg	0.34																				
Na	0.51	0.62																			
K	0.39	0.38	0.52																		
Cl	−0.21	−0.13	−0.03	0.09																	
SO_4	−0.12	−0.02	0.06	0.18	0.85																
HCO_3	−0.11	0.02	0.01	−0.02	0.64	0.66															
CO_3	0.19	0.2	0.34	−0.08	0.15	0.24	0.21														
Ca/Na	−0.13	−0.51	−0.7	−0.35	−0.16	−0.21	−0.04	−0.11													
Ca/Mg	0.365	−0.64	−0.18	−0.11	−0.08	−0.1	−0.05	−0.03	0.403												
SO_4/Cl	−0.042	0.145	0.151	0.215	0.238	0.57	0.109	0.331	−0.218	−0.164											
Temp.	0.23	−0.04	−0.03	−0.07	0.27	0.05	0.07	0.2	0.09	0.23	−0.17										
pH	0.11	0.13	0.2	0.14	0.03	0.08	0.29	0.13	0.05	−0.04	0.03	0.14									
EC	−0.15	0.12	0.08	0.18	0.83	0.89	0.75	0.31	−0.21	−0.18	0.41	0.08	0.08								
NA%	0.333	0.362	0.81	0.405	0.013	0.085	−0.02	0.028	−0.83	−0.14	0.106	−0.11	0.066	0.042							
SAR	0.42	0.53	0.92	0.49	0	0.1	0.02	0.11	−0.7	−0.2	0.16	−0.1	0.19	0.1	0.91						
TH	0.678	0.793	0.748	0.515	−0.18	−0.07	0.013	0.27	−0.44	−0.17	0.086	0.14	0.164	0.029	0.398	0.572					
TDS	−0.03	0.136	0.226	0.227	0.831	0.908	0.846	0.37	−0.27	−0.13	0.393	0.126	0.229	0.907	0.185	0.235	0.125				
SICa	0.03	0.29	0.4	0.24	0.29	0.39	0.62	0.31	−0.23	−0.19	0.14	0.27	0.9	0.38	0.26	0.37	0.32	0.66			
SIdo	−0.12	0.28	0.41	0.26	0.44	0.41	0.57	0.46	−0.34	−0.34	0.14	0.05	0.77	0.42	0.37	0.42	0.16	0.64	0.86		
SIgy	0.197	0.289	0.365	0.251	0.377	0.695	0.09	0.564	−0.31	−0.02	0.678	0.384	0.124	0.423	0.114	0.194	0.503	0.518	0.274	0.234	
$\log pCO_2$	0.088	0.258	−0.026	0.208	−0.105	−0.164	−0.02	0.088	−0.138	−0.084	−0.103	−0.013	−0.56	0.034	−0.038	−0.16	0.327	−0.003	−0.322	−0.246	0.115

tion due to the long residence time of the water in the rock (Fig. 6a, b). There is a highly positive correlation between SO_4^{2-}–TDS (r = 0.91) and SO_4^{2-}–EC (r = 0.89) (Table 3). The EC and TDS values are high in places where the thickness of the alluvium (wells 18, 26, 28) is increased. EC, a reflection of the total ions, can be attributed to the very highly positive correlation (r = 0.91) between EC and TDS values. A low TDS and SO_4^{2-}/Cl^- ratio, and a high Ca^{2+}/Mg^{2+} ratio are observed in the recharge areas (spring Ç-21, and wells 33, 69, 73 and 100), whereas opposite conditions are associated with discharge areas.

There seems to be a relationship between the fluctuation of the groundwater level and the unconfined aquifer (Afşin 1991). The aquifer recharges near well number 69 (Figure 2). Some well waters (2, 52, 52A) are contaminated by the creek and wastes. Wells 18, 28, 44, and 65A (bordered with Tss), and springs Ç-20 and Ç-21 are also contaminated by waste waters, which may result in an increase in SO_4^{2-} values (Fig. 4a, b).

The Ca^{2+}/Mg^{2+} ratio may change only sligthly along short paths of groundwater movement (Tóth 1966). The Ca^{2+}/Mg^{2+} ratios are higher than one unit in the groundwaters in the plain (wells 3, 14, 33, 69, 73, 100, and springs Ç-2, Ç-4, Ç-5, Ç-16A, Ç-21; Fig. 5a, b). Although the observed variation in the Ca^{2+}/Mg^{2+} ratio seems to indicate groundwater flow directions, its high magnitude may also reflect different ratios from the rocks. For instance, the Ca^{2+}/Mg^{2+} ratio is high in the water sampling points near the limestones. There is a reverse relationship between the Ca^{2+}/Mg^{2+} and SO_4^{2-}/Cl^- ratios (r = −0.16).
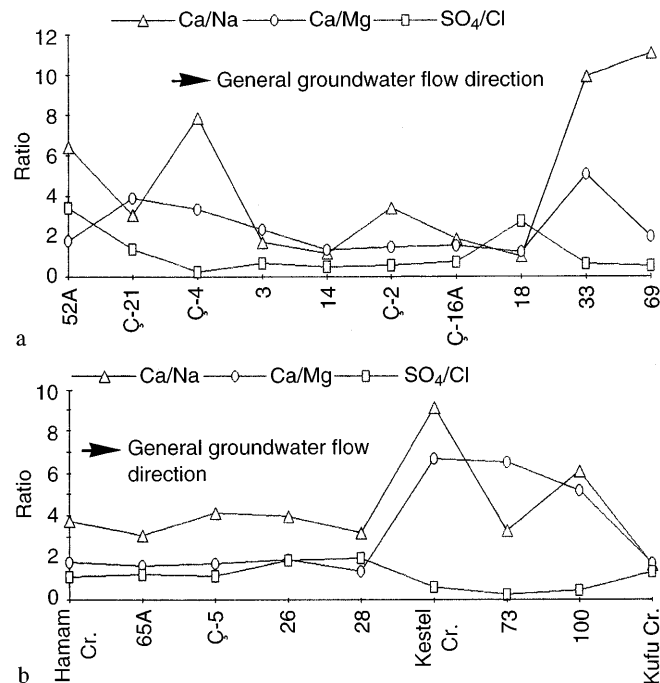

Fig. 5a, b
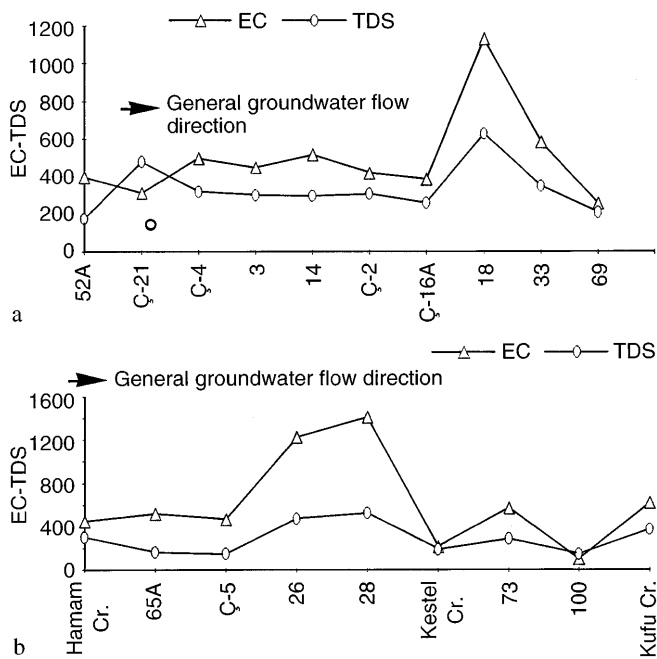Variation of Ca/Mg, Ca/Na and SO_4/Cl ratios along the groundwater flow path (values of the ions are meq/l)

Fig. 6a, b

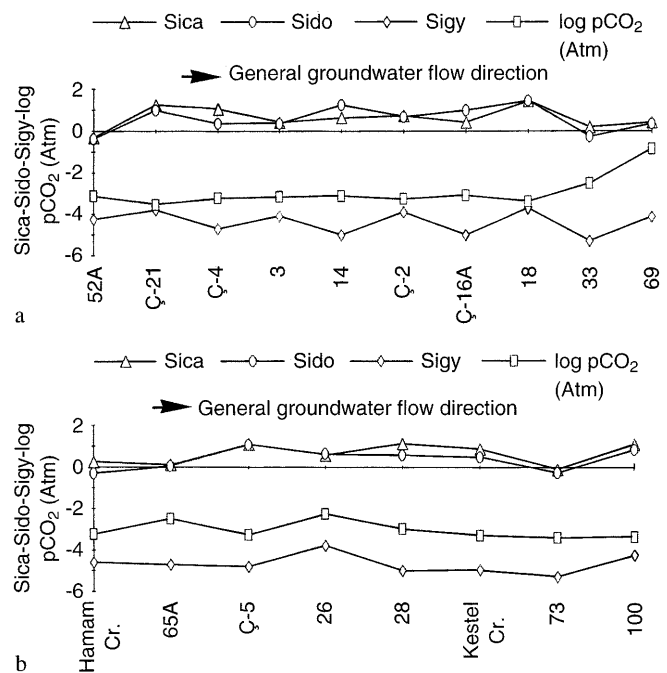Variation between EC (µmho/cm) and TDS (mg/l) values along the groundwater flow path

Fig. 7a, b

Variation of calcite (SIca), dolomite (SIdo) and gypsum (SIgy) saturation index values along the groundwater flow path (units are as in Table 2)
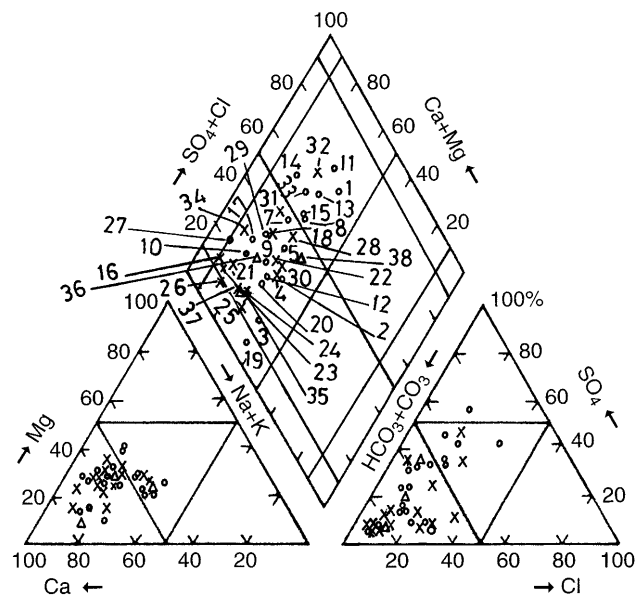
Positive and highly positive correlations between pH and SIdo (r=0.77), pH–SIca (r=0.90), SIca–SIdo (r=0.86), TDS–SIgy (r=0.52), TDS–SIdo (r=0.64), and SO_4^{2-}–SIgy (r=0.70) are present. All waters may generally precipitate calcite in unfavorable physicochemical conditions. There is a negative correlation between pH and logpCO$_2$ (r=−0.56). Some waters (14, Ç-21) may precipitate dolomite, and the water of well 18 saturated with calcite and dolomite (Fig. 7a, b). Increased saturation index values, especially for calcite, may be related to the residence time during low recharge (Scanlon 1989) which gives rise to high ionic concentration along the groundwater flow path.

Hydrochemial Facies

Two hydrochemical facies have been identified as forming through the interaction between rock and water along groundwater flow paths (Figs. 8 and 9): 1) facies Ca–Mg–HCO$_3$, and facies 2) Ca–Mg–SO$_4$–HCO$_3$. The Ca–Mg–HCO$_3$ facies (young waters) occurs mainly in the recharge areas (Ophori and Tóth 1989). This facies is also the most abundant type of water in the plain. HCO$_3^-$ is the major anion and Ca^{2+} and Mg^{2+} are the main cations of this facies. The relative concentrations of the ions occur in the order of $Ca^{2+}+Mg^{2+}>Na^++K^+$, and $HCO_3^->Cl^-+SO_4^{2-}$. This facies may occur during rapid-flow-through times, which results in low ionic concentrations during high recharge in shallow zones, i.e., unconfined aquifer conditions. The Ca–Mg–HCO$_3$-type water may correspond to the upper zone (Freeze and Cherry 1979), which is characterized by active flushing through relatively well-leached rocks, and low TDS values with

Fig. 8

Trilinear Piper diagram showing the hydrochemical groundwater facies (data from Table 2; creek, × spring, ○ well)

high concentrations of HCO$_3^-$, and high Ca^{2+}/Mg^{2+}, and Ca^{2+}/Na^+ ratios, indicative of a shallow system (Figs. 5a, b; 6a, b).

The Ca–Mg–SO$_4$–HCO$_3$ facies is dominant in the intermediate (discharge) areas (Ophori and Tóth 1989). These
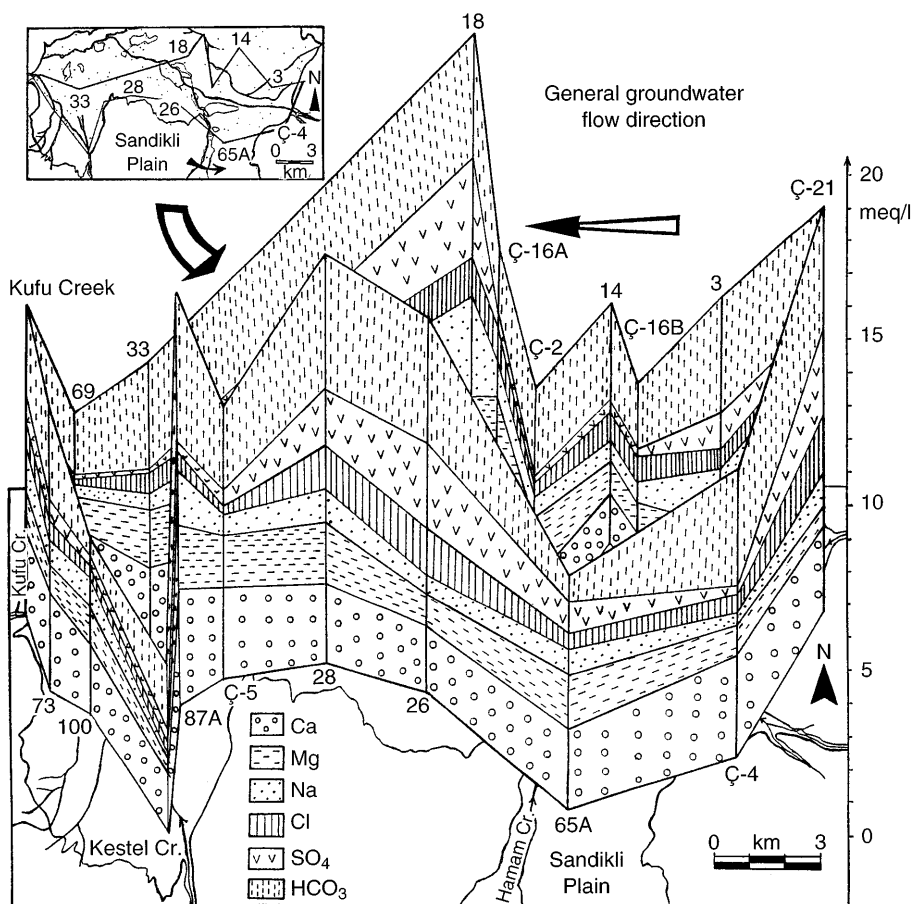
Fig. 9
A panel diagram showing hydrochemical evolution along the groundwater flow path

types of waters, which are mixed or relatively old waters, are found in a narrow area at eight water sampling points in the plain. The major anion is usually SO_4^{2-} and HCO_3^- is the next most frequently occurring anion of this facies. The Ca–Mg–SO_4–HCO_3 facies may result from increased cation exchange and SO_4^{2-} reduction during long residence time associated with low flow. High TDS values, low Ca^{2+}/Mg^{2+} ratio, and high SO_4^{2-} and HCO_3^- concentrations mark the discharge areas. Increased residence time during low recharge produces higher ionic concentrations with $Ca^{2+} + Mg^{2+} > Na^+ + K^+$, and $SO_4^{2-} + Cl^- > HCO_3^- + CO_3^{2-}$. The Ca–Mg–$SO_4$–$HCO_3$ facies water, with a less active groundwater circulation and higher TDS and SO_4^- values, may correspond to the intermediate zone (Freeze and Cherry 1979).

Water Quality

Water quality and utilization may be discussed in view of physical, chemical, and biological parameters (Davis and DeWiest 1966); the hydraulic regime and type of the flow system (Tóth 1984); and the hydrogeological properties of recharge and discharge areas. There are different water quality standards for the various uses of water. The results of the chemical analyses show that the groundwater in the study area is chemically potable and suitable for domestic purposes, i.e., drinking and household uses, since the various ionic concentrations and parameters are generally within the maximum acceptabile limits of the WHO (1984), TSI (1986) and WPA (1988), guidelines (Table 4). The groundwater in the plain is excellent for irrigation with a medium salinity hazard. The Salinity hazard for some water wells and springs is classified as high (2, 18, 26, 28) and a few show very high salinity contamination (Ç-20 and 52, Table 5).

Sodium concentration is important when evaluating the suitability of groundwater for irrigation because sodium may cause an increase in the hardness of the soil as well as a reduction in its permeability (Tijani 1994). The Na % and SAR values are generally low and intermediate in the groundwaters around volcanic and metamorphic areas (Table 5a, b). There is a highly positive correlation between Na % and SAR (r=0.91). Quality values (Na %, TH = Total Hardness, SAR) decreased slightly towards Kufu creek along the groundwater flow path. The TH values of the waters are high at some water points (wells 2, 3, 18, 18A, 87A) (Table 6). A highly positive correlation (r=0.80) is obtained between TH values, and Ca^{2+} and Mg^{2+} (Table 2).

Table 4
Comparison of the chemical parameters of the groundwaters in the study area to different water quality standards

Parameter	Range	Mean	WHO (1984)	TSI (1986)		Water Pollution Control Act (1988)
				spring waters	drinking waters	
Temperature (°C)	8 – 15	11.2	—	—		I
pH	7.1 – 8.8	8.2	6.5–8.5	7.0–8.5	6.5– 8.5	I
EC (μmho/cm)	106 –2018	610	1400	—	—	—
Ca^{++} (mg/l)	20 – 80	48.8	200	25	75 –200	—
Mg^{++} (mg/l)	3.6 – 32.4	18.4	—	10	50 –150	—
Na^{+} (mg/l)	3.91– 271.4	27.0	200	—	—	I
K^{+} (mg/l)	0.39– 35.1	4.8	—	—	—	—
Cl^{-} (mg/l)	6.67– 138.45	28.84	250	30	200 –600	I–II (52 and Ç-20)
SO$_4^{-}$ (mg/l)	4.99– 424.32	56.0	400	20	200 –400	I (52 III and Ç-20 IV)
HCO$_3^{-}$ (mg/l)	31.72– 516.06	178.0	—	—	—	—
TDS (mg/l)	116.48–1097	348.6	1000 g/l	500	1500	I–II (18, 28, 52, Ç-20)

Table 5
a Salinity hazard and the relationship between SAR and EC for the groundwaters in the study area, and **b** suitability of the groundwaters for irrigation in the study area

Table 5a

SAR	EC (μmho/cm)	Water class	Spring	Well	Creek	Salinity hazard
	250	excellent		76, 100	Kestel	low
<10	251–750	good	Ç-2, Ç-2B, Ç-4, Ç-5, Ç-7, Ç-9, Ç-10, Ç-16A, Ç-16B, Ç-17, Ç-18, Ç-21, Ç-28, Ç-29	3, 14, 15, 18A, 33, 35, 44, 51, 52A, 65A, 69, 73, 87A	Hamam Kufu	middle
	751–2000	permissible		2, 18, 26, 28		high
	>2000	doubtful	Ç-20	52		very high

Table 5b

Na %	Water class	Spring	Well	Creek
20	excellent	Ç-2, Ç-2B, Ç-4, Ç-5, Ç-7, Ç-9, Ç-10, Ç-16B, Ç-18, Ç-20, Ç-21, Ç-28, Ç-29	26, 28, 33, 35, 44, 52, 52A, 65A, 69, 76	Kestel Hamam
21–40	good	Ç-16A, Ç-17	2, 3, 14, 15, 18, 18A, 51, 73, 87A, 100	Kufu

Table 6
Classification for total hardness (TH) of the groundwaters in the study area

Hardness	Water class	Spring	Well	Creek
0–10	drinking water	Ç-10, Ç-18	76, 51	
11–22	fresh water	Ç-2, Ç-2B, Ç-4, Ç-5, Ç-7, Ç-16A, Ç-16B, Ç-17, Ç-20, Ç-21, Ç-28, Ç-29	14, 15, 26, 28, 33, 35, 44, 52, 52A, 65A, 69, 73, 100	Kestel Kufu
23–32	hard water		2, 3, 18, 18A, 87A	Hamam

Conclusions

1) An open system is demonstrated for the alluvium aquifer in the plain.

2) The chemical pattern correlates with the flow pattern of groundwater in the plain (unconfined aquifer).

3) A high Ca^{2+}/Mg^{2+} ratio and high HCO_3^- concentration; and low TDS and SO_4^{2-} concentrations orrur in recharge areas, whereas opposite trends for these parameters are associated with discharge areas.

4) The length of time during which the groundwater contacts the aquifer material is an important factor in the development of ionic concentration.

5) The Ca–Mg–HCO_3 facies waters dominating the recharge areas are young, shallow waters whereas the Ca–Mg–SO_4–HCO_3 facies waters which are shallow, mixed, and relatively old (Chebotarev 1955), dominate the discharge areas.

6) Ionic concentrations, TDS, EC and water quality suggest that groundwater residence time is primarily controlled by the occurence of different hydrochemical facies (water types). Different water types and residence times are attributed to the hydrogeologic properties (porosity, permeability and homogeneity) of the unconfined aquifer formation.

7) The hydrochemical results relatively conform with the Chebotarev (1955) sequence.

8) Groundwaters and creek waters in the plain are, in general, chemically potable and suitable for both domestic and agricultural purposes.

References

Afşin M (1991) Hydrogeological study of the Kuruçay plain and the Hudai bath (Sandıklı-Afyon/Turkey). Unpublished Ph. D. thesis. Ankara: Institute of Pure and Applied Science, Ankara University. 330 pp (abstract in English)

Afşin M and Baş H (1996) Hydrochemical evaluation of the Koçpınar springs (Aksaray), Central Anatolian, Turkey. Geol Bull Turk 39:(in press)

Appelo CAJ and Postma D (1992) Groundwater, geochemistry and pollution. Amsterdam: Vrije Universiteit. 510 pp

Back W (1960) Origin of hydrochemical facies and groundwater in the Atlanlic coastal plain. Report xxı. Int. Geol. Congress, Nordlend pt. 1, 87 p

Bayari CS and Kurttaş K (1995) Geochemistry of regional groundwater flow in the Aladağ karstic aquifer, Eastern Taurids-Turkey: effect of flow conditions. Doğa, Turk J Earth Sci 4:29–37

Chebotarev II (1955a) Metamorphism of natural waters in the crust of weathering: part I. Geochim Cosmochim Acta 8:22–48

Chebotarev II (1955b) Metamorphism of natural waters in the crust of weathering: part II. Geochim Cosmochim Acta 8:137–170

Chebotarev II (1955c) Metamorphism of natural waters in the crust of weathering: part III. Geochim Cosmochim Acta 8:198–212

Davis SN and DeWiest RJM (1966) Hydrogeology. New York: John Wiley & Sons. 463 pp

Domenico PA (1972) Concepts and models in groundwater hydrology. New York: McGraw-Hill

Domenico PA and Schwartz FW (1990) Physical and chemical hydrogeology. New York: John Wiley & Sons. 824 pp

Freeze RA and Cherry JA (1979) Groundwater. Englewood Cliffs, NJ: Prentice-Hall, 604 pp

Ophori DU and Tóth J (1989) Patterns of groundwater chemistry, Ross Creek basin, Alberta, Canada. Ground Water 27(1):20–26

Scanlon BR (1989) Physical control on hydrochemical variability in the Inner Bluegrass karst region of Central Kentucky. Ground Water 27(5):639–646

Schoeller H (1962) Les Eaux Souterraines. Paris: Mason et Cie. 642 pp

Tijani J (1994) Hydrochemical assessment of groundwater in Moro area, Kwara state, Nigeria. Environ Geol 24:194–202

Tóth J (1966) Groundwater geology, movement chemistry and resources near Olds, Alberta. Res Coun of Alberta Bull 17

Tóth J (1984) The role of regional gravity flow in the chemical and thermal evolution of groundwater. Proc First Canadian/American conference on hydrogeology, Banff. Alberta Turkish Standard Institution (1986) Drinking Water. Standard No. 266, Ankara (In Turkish) 97 p

WHO (1984) Guidelines for drinking-water quality, vol. 1, Recommendations. Geneva: WHO, 130 pp

Water Pollution Control Act (1988) Turkish Offical Gazette, 4 September, I.19919, 13–73 (In Turkish)